RIVER RESEARCH AND APPLICATIONS

River Res. Applic. **22**: 631–649 (2006)

Published online 11 April 2006 in Wiley InterScience
(www.interscience.wiley.com). DOI: 10.1002/rra.925

DETERMINATION OF BANK ERODIBILITY FOR NATURAL AND ANTHROPOGENIC BANK MATERIALS USING A MODEL OF LATERAL MIGRATION AND OBSERVED EROSION ALONG THE WILLAMETTE RIVER, OREGON, USA

JENNIFER ROSE WALLICK,[a]* STEPHEN T. LANCASTER[b] and JOHN P. BOLTE[c]

[a] *DHI, Inc., 319 SW Washington St., Suite 614, Portland, Oregon 97204, USA*
[b] *Department of Geosciences, Oregon State University, USA*
[c] *Department of Bioengineering, Oregon State University, USA*

ABSTRACT

Many large rivers flow through a variety of geologic materials. Within the span of several kilometres, bends may alternately flow against recently reworked sediments, older, more indurated sediments or highly resistant materials. As sediment size, cementation, and other properties strongly influence the erodibility of river banks, erosion rates and channel planform are likely to vary significantly along the length of large rivers. In order to assess the role of bank materials on bank erosion rates, we develop a method for detecting relative differences in erodibility between bank materials along large floodplains. By coupling historic patterns of channel change with a simple model of bank erodibility we are able to track relative changes in bank erodibility among time intervals and bank materials. We apply our analysis to the upper Willamette River, in northwestern Oregon for three time periods: 1850–1895, 1895–1932 and 1972–1995 and compute relative differences in bank erodibility for Holocene alluvium, partially cemented Pleistocene gravels, and revetments constructed in the 20th century. Although the Willamette is fundamentally an anastomosing river, we apply the model to single-thread portions of the channel that evolved through lateral migration. Our simple model of bank erodibility reveals that for all three-time periods, banks composed of Holocene alluvium are at least 2–5 times more erodible than banks composed of Pleistocene gravels. Revetment installed in the 20th century is highly resistant to erosion and is at least 10 times less erodible than Pleistocene gravels. Copyright © 2006 John Wiley & Sons, Ltd.

KEY WORDS: bank erosion; Willamette River; bank materials; meander migration

INTRODUCTION

Society has a need for understanding the controls on lateral migration of rivers, especially those flowing through densely populated areas. Although channel stabilization efforts may be necessary to support a growing array of agricultural and urban communities, such actions reduce a river's creation of new geomorphic surfaces. Processes, such as bank erosion, gravel-bar deposition and side-channel maintenance promote healthy aquatic and riparian ecosystems by hyporheic flows, recruitment of woody vegetation, and creation of off-channel habitat (Dykaar and Wigington, 2000; Fernald *et al.*, 2001; Landers *et al.*, 2002). Restoring natural floodplain functions while protecting community investments requires a strategy that addresses both intrinsic and anthropogenic controls on bank erodibility.

Several studies have used simple models of meander migration to predict channel movement and bank erosion along low-gradient streams (Johannesson and Parker, 1985; Garcia *et al.*, 1994). Subsequent authors (e.g Micheli and Kirchner, 2002; Micheli *et al.*, 2004) have used a similar approach to quantify the relationship between bank erodibility and riparian vegetation for stream reaches characterized by homogeneous riparian vegetation. To better understand how resistant bank materials influence channel migration along large floodplains (i.e. tens of

*Correspondence to: J. R. Wallick, DHI, Inc., 319 SW Washington St., Suite 614, Portland, OR 97204, USA. E-mail: rwa@dhi.us

Contract/grant sponsor: National Science Foundation; contract/grant number: 0120022.

Received 1 December 2004
Revised 15 September 2005
Accepted 21 October 2005

Copyright © 2006 John Wiley & Sons, Ltd.

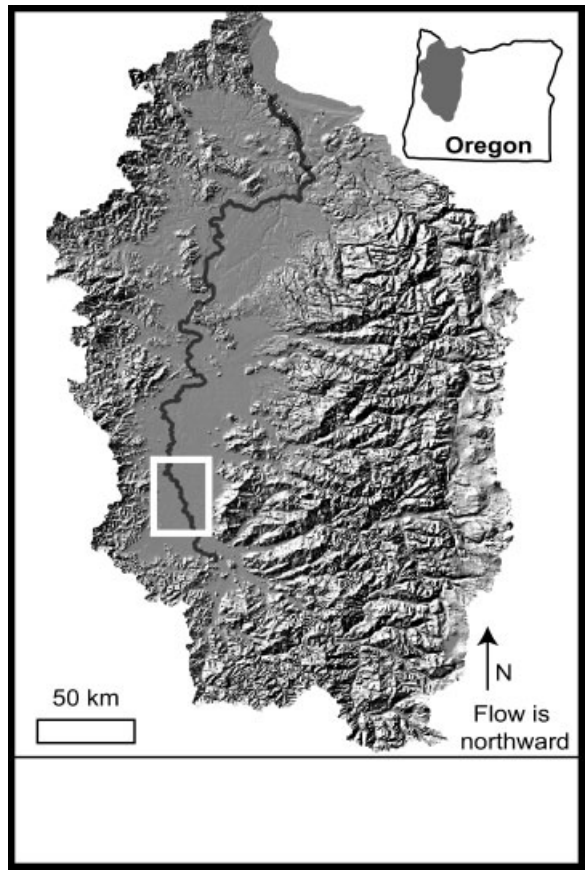

Figure 1. Willamette River Basin in northwestern Oregon. Box indicates upper Willamette study area

kilometres), we adapt the methodology of Micheli and Kirchner (2002) to quantify bank erodibility at the scale of individual bends for rivers with heterogeneous bank materials.

Along the upper Willamette River in northwestern Oregon (Figure 1), resistant bank materials appear to have exerted an increasingly important role in channel evolution. In the mid-19th century, the upper Willamette was a dynamic, anastomosing stream flanked by loosely consolidated Holocene sediments. In contrast, the modern Willamette largely evolves through meander migration, yet much of the channel is presently flowing against naturally resistant Pleistocene gravels or bank stabilization structures (revetments) (Figure 2). Historical migration rates have fluctuated as the Willamette has transitioned from an anastomosing stream characterized by frequent avulsions to a more stabilized stream dominated by lateral migration, and it is unclear how the distribution of resistant bank materials has influenced historical channel change. Although Pleistocene gravels appear more consolidated than Holocene alluvium, it is uncertain whether differences in bank erodibility between naturally occurring materials can be detected and how the erodibility of naturally resistant materials differs from revetments. It is also unknown whether the relative differences in bank materials have remained constant over time.

By linking historic records of channel change with patterns of bank erodibility we quantify the roles that resistant bank materials have played in determining channel change along the upper Willamette between 1850 and 1995. Our bank erodibility analysis provides a mechanism for tracking changes in erodibility over time, and detecting relative differences in erodibility between materials. Such a strategy enables us to determine which areas of the floodplain are intrinsically more erodible than others and may provide a framework for field-based bank strength analyses and future restoration strategies.

Copyright © 2006 John Wiley & Sons, Ltd.

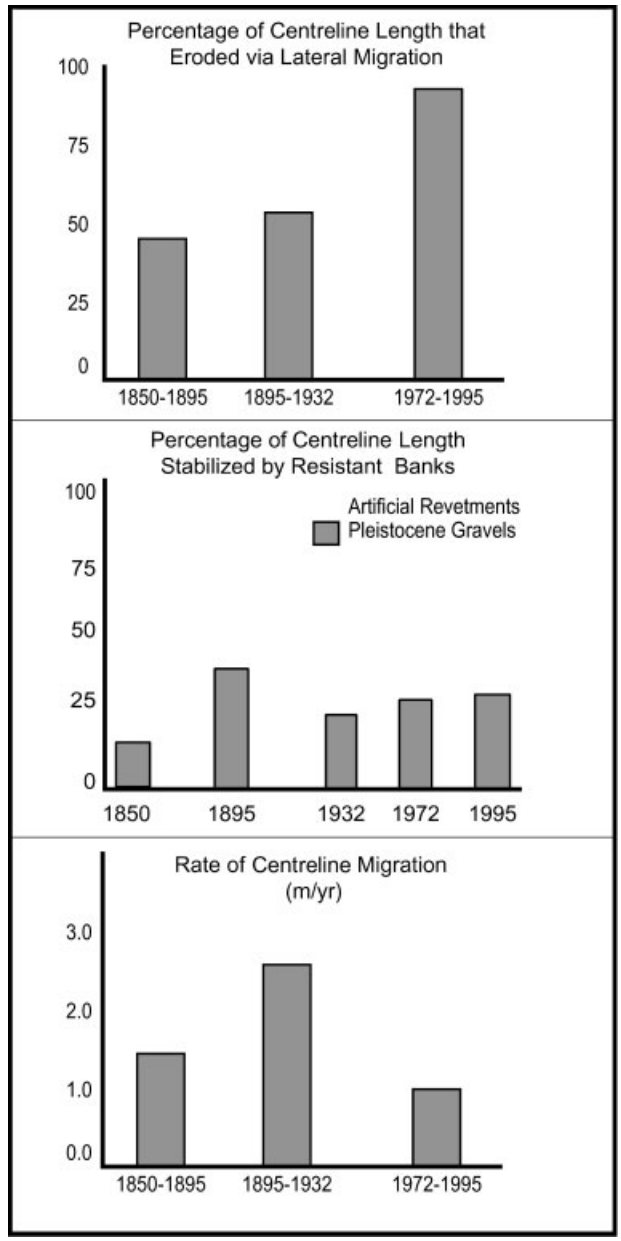

Figure 2. Migration patterns for upper Willamette 1850–1995. Large increases in both the lengths of channel prone to lateral migration and the length of resistant banks are accompanied by fluctuating migration rates

WILLAMETTE RIVER STUDY AREA

The Willamette River is a large alluvial river draining a 29 800 km^2 basin in northwestern Oregon (Figure 1). The rugged and volcanically active Cascade Range forms the eastern boundary of the Willamette Basin, and the Oregon Coast Range forms the western boundary. The headwaters and major tributaries of the Willamette primarily drain the steep, degrading landscapes of the Cascade and Coast Ranges and differ sharply from the low-gradient, meandering streams of the valley-floor sedimentary basin. The mainstem Willamette begins at the confluence of the Coast and Middle Forks of the Willamette in the southern valley and flows northward for more than 300 km to its confluence with the Columbia River. The Willamette Valley is characterized by Mediterranean climate with cool,

Copyright © 2006 John Wiley & Sons, Ltd.

wet winters and warm, dry summers. Average precipitation in the valley floor is approximately 120 cm per year, which falls mainly as rainfall during the winter (Oregon Climate Service, 2004).

We conducted our study along the upper 30 km of the Willamette River floodplain between the confluences of the McKenzie and Long Tom Rivers, or according to the floodplain-based reference frame of Hulse *et al.* (2002), between floodplain kilometres (FPKM) 216 and 187 (Figure 3). Within the study area, the Willamette is

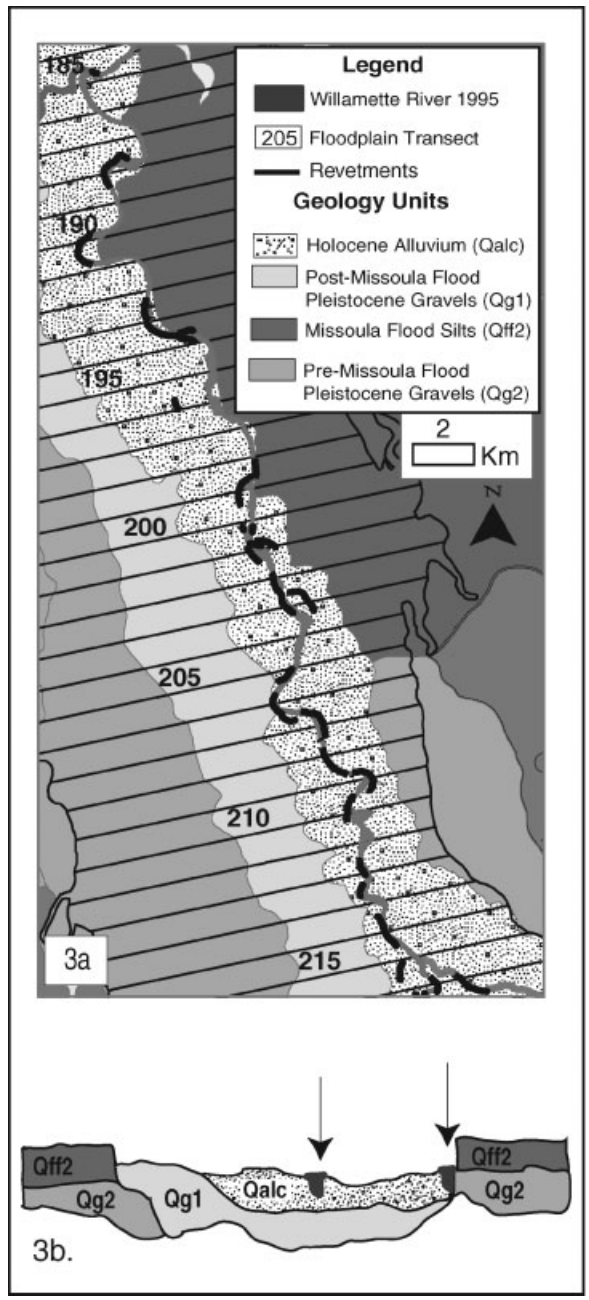

Figure 3. Upper Willamette study area. (a) Geologic setting of upper Willamette. Primary bank materials are Holocene Alluvium and Pleistocene Gravels, which underlay Missoula Flood Silts. Revetments are presently used to stabilize more than 40% of the channel. (b) Generalized cross section of Willamette floodplain. Arrows indicate typical locations of Willamette River within Holocene floodplain

Copyright © 2006 John Wiley & Sons, Ltd.

predominantly an anastomosing stream in which flow was historically separated by large (1–10 km^2), semi-stable, forested islands. According to 19th century Corps of Engineer reports:

> Each year new channels are opened, old ones closed; new chutes cut, old ones obstructed by masses of drift; sloughs become the main bed, while the latter assume the characteristics of the former; extensive rafts are piled up by one freshet only to be displaced by a succeeding one; the formation of islands and bars is in constant progress. . . .
> (pg 766, Annual Report of the Chief of Engineers, (USACE, 1875).

Channel stabilization efforts have typically confined flows in the modern Willamette to a single channel, and the river primarily evolves through lateral migration (Figure 2). However, the floodplain retains many relict features characteristic of a multi-thread planform, and some side channels remain active during high flows. Channel shifting in the late 20th century was more subtle than for historic periods; migration primarily occurred along areas unconfined by revetment and avulsions generally took place along secondary channels.

The Willamette Basin is blanketed with a series of Quaternary deposits that form three distinct types of bank materials in the study area (Figure 3). Indurated Pleistocene gravels (Qg2 map unit) were deposited as broad braidplains and crop out along the right bank in the middle and lower study reach (O'Connor *et al.*, 2001). Between 15–12.7 ka, a series of catastrophic Missoula Floods back-filled the Willamette Valley, creating a lacustrine setting in which fine-grained sediments (Qff2) were deposited atop Qg2 gravels. As the Missoula Floods entered the Willamette Valley from the north, Qff2 thins southward, extending to FPKM 206 in the study area. Where Missoula Flood sediments form the surficial geological unit, Holocene incision exposes Qg2 gravels at river level such that flows interact with Qg2 rather than Qff2 during all but exceptionally high discharges. The Holocene floodplain (Qalc map unit) of the Willamette is inset within Pleistocene deposits, forming a 2–4 km wide surface that borders the channel on one or both banks for much of the study area. Large boulders (or revetments) emplaced by the Army Corps of Engineers in the 20th century form the third type of bank material and are primarily used to stabilize banks composed of Qalc.

The Pleistocene Qg2 unit forms a uniform layer of sands and gravels deposited in a braided channel system and partially cemented by clay, calcite and iron oxide accumulation (Glen, 1965; Balster and Parsons, 1969; O'Connor *et al.*, 2001). Exposures of Qg2 at river level are nearly vertical and reveal 2–3 m of cobbly gravel fining upward into sand and silt, which is overlain by a 1–2 m-thick paleosol (O'Connor *et al.*, 2001). Within the study reach, the uppermost surface of the Qg2 gravel layer is approximately level with modern bankful stage, while the fine-grained layers generally rise slightly above bankful (as determined during field observations). Though the entire Qg2 unit may range in age from 0.42 Ma to 15 ka, the top of the unit was probably deposited 23–27 ka (O'Connor *et al.*, 2001).

Within the Qg2 gravel layer, individual clasts generally range upto 10 cm in diameter, and sands tightly fill the interstices. Disaggregation Qg2 gravels requires substantially more effort than for Qalc deposits and generally involves the use of implements (such as a rock hammer) to physically separate clasts. Fluvial erosion into Qg2 causes large scour holes to form along the bank toe. Missoula Flood deposits overlaying Qg2 are undermined by this scouring and frequently collapse through slab-type failures.

In contrast to indurated Qg2 gravels, Holocene alluvium encompasses a variety of young ($<$7000 years) surfaces composed of unconsolidated silts, sands and gravels (Balster and Parsons, 1968; O'Connor *et al.*, 2001). Coarse deposits of cobbles and gravels near the active channel fine towards sands, silts and clays with increasing elevation. Modern floodplain surfaces bordering the channel typically rise 1–4 m above the low-water line and are composed of sandy, poorly formed soils capped by thin layers of silts (Balster and Parsons, 1968; Reckendorf, 1973). While there is a great diversity of Qalc surfaces, from recent point bars to forested floodplains, Qalc deposits are all generally poorly to weakly consolidated. Casual digging or scraping can easily disturb Holocene deposits, and even the most seemingly indurated exposures can be loosened by hand.

Historic and recent accounts indicate that the low bank height and loosely consolidated structure of Holocene Alluvium support high rates of erosion (USACE, 1867-1892; Balster and Parsons, 1968). Along unstabilized areas of the modern channel, both forested and non-vegetated banks composed of Qalc frequently erode at modest discharge levels.

In the 1930's the Corps of Engineers began a concerted effort to stabilize rapidly eroding banks with revetments. By 1972, nearly 50% of the channel length in the study area was stabilized, with the majority of revetment

Copyright © 2006 John Wiley & Sons, Ltd.

emplaced along banks composed of Qalc (Figure 3). Although there are several types of revetment used to stabilize banks, much of the revetment consists of large (~1 m in diameter) angular basaltic boulders extending from the bank toe to the top of the bank (Willingham, 1983; Gregory *et al.*, 2002).

DETERMINING PATTERNS OF BANK ERODIBILITY

Model of bank erosion

The rates of bank erosion and (assuming a constant channel width) meander migration are the product of bank erodibility and near-bank streamflow erosivity. While erodibility is an intrinsic material property resulting from characteristics, such as grain size and degree of cementation, erosivity depends upon hydraulic factors including discharge and channel curvature. Given a constant discharge, the product of erodibility and erosivity varies with planform and bank materials, both of which can vary substantially downstream such that bank erosion rates can be highly variable. In order to detect relative differences in erodibility between bank material types and time intervals, we must independently determine the erosivity of near-bank streamflow.

In a perfectly straight channel with a perfectly symmetrical cross-section, the fastest flow will follow the channel centreline. In curved channels, which usually have asymmetrical cross-sections, secondary flows tend to steer the fastest flow towards the bank at the outside of the bend. Near-bank streamflow erosivity is highest where the flow near that bank is fastest. Following (Ikeda *et al.*, 1981), we adapt a model of meander migration whereby bank erosion rate, $\dot{B}_e$, is the product of bank erodibility, E_o, and the deviation, U'_b, of the near-bank flow velocity from the reach-average velocity:

$$\dot{B}_e = E_o * U'_b \tag{1}$$

Bank erosion rate ($\dot{B}_e$) is measured in metres per year, while near-bank flow velocity is calculated in metres per second. When bank erosion rate is converted to metres per second, bank erodibility (E_o) becomes a dimensionless parameter, though values are typically quite small (on the order of 10^{-7}). Actual flow velocity near a particular bank is the sum of reach-average flow velocity, U, and the near-bank velocity perturbation (U'_b), which is generally defined as the solution for the velocity perturbation near one bank (Ikeda *et al.*, 1981). When velocity is higher near the other bank, U'_b is negative, thus the sign of U'_b indicates which bank is experiencing the higher flow velocity.

For a given bend, the magnitude of the near-bank velocity perturbation will be greatest where the fastest flow appears to impinge against one bank, typically at the outside of the bend. Among bends, although the expression for U'_b is complicated (see Appendix), the near-bank velocity perturbation is usually greater in bends with greater curvature and, therefore, greater secondary flow strength. As shear stress at a flow boundary is given by the boundary-normal gradient of flow velocity, shear stress at a channel bank is greatest where the near-bank flow is fastest (i.e. where the magnitude of U'_b is greatest). Therefore, our usage of near-bank velocity serves as a proxy for near-bank shear stress.

According to the hydraulic model of (Johannesson and Parker, 1989), U'_b is a function of both local and upstream curvature. We may therefore calculate U'_b from hydraulic parameters and a map of the channel centreline at a particular time (see Appendix). We assume that the bank erosion apparent from a subsequent channel planform is, within reasonable limits, predicted by the product of E_o and U'_b at that earlier time. Given the observed bank erosion rate between two times and the calculated U'_b, we can solve for bank erodibility:

$$E_o = \frac{\dot{B}_e}{U'_b} \tag{2}$$

where $\dot{B}_e$ is the observed bank erosion rate, and E_o is the inferred bank erodibility. Conceptually, the U'_b calculated from the planform 'normalizes' the observed migration rates so that we can isolate planform characteristics from bank material properties in explaining bank erosion.

Historic channel change

Bank erodibility is calculated using historic maps of the Willamette River for three intervals: 1850–1895, 1895–1932, and 1972–1995. The first interval, 1850–1895, was marked by the initial settlement and development of the

Copyright © 2006 John Wiley & Sons, Ltd.

Table I. Channel maps used in bank erodibility model

Channel maps				
Map date	Original survey or photo source	Map description	Source for georeferencing and digitizing	Precision
1850	General Land Office (GLO) Cadastral Surveys	Cadastral survey of townships and sections. Most of study area surveyed 1851–1853.	Hulse *et al.* (2002)[a]	±10 m
1895	Army Corps of Engineers (USACE)	Navigational blue-line survey. Study area surveyed October–November of 1894.	Hulse *et al.* (2002)	Unknown
1932	USACE	Navigational survey of study area conducted 1931–1932.	Hulse *et al.* (2002)	±5 m
1972	USACE	Main channel and active channel[b] digitized from mosaic of orthophotographs in 1972 Willamette River and Tributaries Map Book. Photography flown May 2, 1972 at ~300 cms.	These authors	± 10 m
1995	USACE	Main channel and active channel[b] digitized from orthophotographs flown August 1994 and September 1995 (~150–200 cms).	Spencer Gross Photography, PNWERC & these authors	±5 m

[a]Pacific Northwest Ecosystem Research Consortium (PNWERC) presented in Hulse *et al.* (2002).
[b]For 1972 and 1995 we digitized both the actual water surface boundary and the active channel from aerial photographs. Although discharge at the time the 1972 photos were taken is about twice that of flow during the 1995 photos, there is little difference in the stage-discharge relationship for these flows (~1 m) and reach-averaged channel width for the low-water channel varies by less than 2% between the photo series.

Willamette Valley. Although the US Army Corps of Engineers (USACE) began channel improvements in 1875, much of the floodplain was forested and the channel was highly dynamic throughout the interval. During the second interval, 1895–1932 navigational improvements to the channel continued, but the floodplain remained largely undeveloped. The interval 1932–1972 is excluded from analysis because extensive revetments and seven upstream flood-control dams were constructed during this period (Figure 2). The last interval, 1972–1995, provides insight into channel dynamics following this regulation and stabilization.

Digital historic maps of the Willamette River were compiled from survey data and aerial photographs (Table I). For 1850, 1895 and 1932, we used maps of the active channel produced by the Pacific Northwest Ecosystem Research Consortium (PNWERC) from surveys conducted by the General Land Office in 1850 and USACE in 1895 and 1932 (Hulse *et al.*, 2002). For the historic maps and the aerial photos, the active channel was defined as the area within the boundaries of the annual high water (1–2 year flow), although definition of these boundaries was sometimes subjective. Where present, steep banks defined more objective active channel boundaries. Gravel bars, small side channels and surfaces vegetated with annual species (e.g. small shrubs, grasses and willows) were included within the active channel, and channel-adjacent areas and islands containing larger woody vegetation were excluded (Gregory *et al.*, 2000).

In our analysis, we were primarily concerned with channel dynamics related to the main thread of flow and edited our 1972 and 1995 maps, accordingly. For 1972 and 1995, when the channel was relatively stable, we mapped both the 'active' and 'main' channels from aerial photos produced by the USACE (Table I). Whereas the active channel contained gravel bars, side channels and other features within the annual high-water boundaries, the main channel was defined by the wetted perimeter of the largest channel. Using aerial photography, we edited the 1995 active channel map produced by the PNWERC so that the 1995 and 1972 active channel maps were consistent with our aim to primarily consider dynamics associated with the main channel.

In much of the late-20th-century floodplain, the main and active channels were nearly identical because bank stabilization and vegetation encroachment allowed the channel to adopt a well-defined planform varying little

Copyright © 2006 John Wiley & Sons, Ltd.

with fluctuations in discharge. However, several dynamic reaches have a very wide active channel containing multiple gravel bars and side channels. In these areas, the centreline of active-channel often appeared to shift over time (typically due to narrowing and vegetation encroachment) though actual bank erosion was negligible. Thus, the boundaries of the main channel at relatively low water provide a more precise delineation of the channel and allow for more accurate bank erosion measurements.

We assume that because the active channel marks the boundaries of annual highwater, the active channel approximates the 'bankfull' channel. Because we calculate U'_b for bankfull discharge, channel width measurements and centreline digitization for all time periods are primarily based on the active channel (Table I). Measurements of bank erosion are based on active-channel boundaries for 1850, 1895 and 1932, and on the more accurate main-channel boundaries for 1972 and 1995.

Calculating bank erosion rates ($\dot{B}_e$)

The objective of our analysis is to interpret bank erosion at the scale of individual bends by linking U'_b with adjacent bank materials. We use 'bend-scale polygons' as a basis for defining spatially-explicit areas of channel change (Figure 4). Migration during each time interval is interpreted from two channel planforms bracketing that interval. For each pair, the latter planform was divided into a series of polygons defining bends and straight sections. Each polygon was classified with information according to the style of change, whether avulsion or lateral erosion, and a preliminary measurement of the erosion distance. Bends experiencing great erosion (e.g. >300 m) were

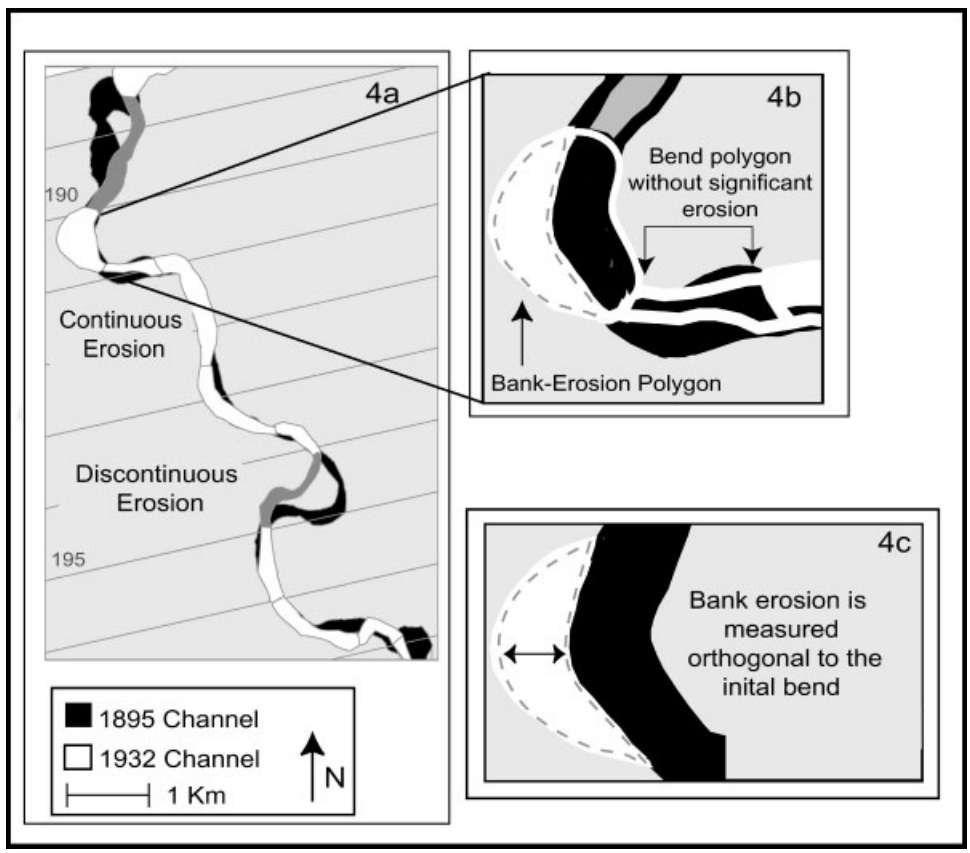

Figure 4. Calculating bank erosion rates with bend-scale and bank-erosion polygons. (a) The channel was divided into contigous bend-scale polygons classified according to magnitude and style of erosion. Bends that experienced continuous erosion (e.g. moderate lateral migration) were selected for our analysis. Bends that experienced discontinous erosion (e.g. avulsion or extreme migration with >500 m of erosion) were excluded. (b) For bends with significant erosion (i.e. >10 m), eroded areas define bank-erosion polygons. (c) Average bank length is defined as half the perimeter of the bank-erosion polygon and bank erosion (a distance) is the ratio of polygon area to average

Copyright © 2006 John Wiley & Sons, Ltd.

excluded from the present analysis because the model can only characterize relatively small, incremental changes. Avulsing reaches were excluded because the model can only characterize continuous migration.

Bank erosion distances were calculated from areas and perimeters of bank-erosion polygons outlining the actual bank area eroded for each bend (Figure 4):

$$B_e = \frac{2A}{P} \tag{3}$$

where, B_e is the average distance of bank erosion perpendicular to the channel; A is the area of the bank-erosion polygon; P is its perimeter; and $P/2$ is the average bank length for the time period. Bank erosion rates are calculated by dividing the distance migrated by the time interval:

$$\dot{B}_e = \frac{B_e}{T} \tag{4}$$

where, T is the time interval in years, which is converted to seconds.

Similar studies of channel change have calculated migration rates by overlaying channel centrelines from two time periods (Nanson and Hickin, 1986; Micheli and Kirchner, 2002; O'Connor *et al.*, 2003). This approach is unsuitable for the Willamette River because significant changes in channel width between 1850 and 1995 (Wallick, 2004) cause centreline migration rates to misrepresent bank erosion rates.

Calculating near-bank stream velocity perturbations (U_b')

We use the near-bank velocity model of (Johannesson and Parker, 1989) to calculate U_b' for points placed along the centreline during each time period (Appendix). The maximum value of U_b' associated with each bend-scale polygon is our surrogate for near-bank flow erosivity in Equation (2). The JP model was derived using conservation of fluid momentum and mass for both streamwise and cross-stream directions. In addition to local and upstream curvature, bed topography is addressed through the coupling of transverse bedslope with effective curvature (a weighted average of upstream and local curvature). In this manner the JP model accounts for the phenomenon that maximum transverse bedslope, (i.e. the slope between the top of the point bar and the bottom of the pool), generally occurs slightly downstream from the point of maximum curvature.

Upon adaptation of the equations presented in Johannesson and Parker (1989), the model becomes more representative of the Willamette River. Our first adaptation is the usage of a formula for transverse bed slope in gravel bed rivers developed by Ikeda, 1989, (Appendix). Additionally, we found that the JP model is sensitive to small planform irregularities, which can be introduced by both natural fluctuations in centreline position and the digitization process. We used smoothed local curvature, calculated from a 5-point moving average of local curvature, to calculate effective curvature and U_b'. After smoothing local curvature we obtained more realistic results than those produced in non-smoothed trials.

The JP model calculates effective curvature and U_b' for points placed along the channel centrelines digitized from historic maps and aerial photographs (Table I). Points were placed every 50 m along the centreline. During all time periods, reach-average channel width was greater than 150 m, so centreline points are spaced at less than every one-third channel width.

The JP model requires reach-average width, average depth at bankfull discharge, median bed material grain size and valley slope (Table II). For each time period, reach-average width of the active channel was measured from transects drawn perpendicular to the downstream direction at 1 km intervals (Table II). Reach-average bankfull flow velocity for 1995 was calculated from discharge, depth (both from USACE records), and width (measured from the 1995 active channel) at bankfull flow at the Harrisburg gauge (FPKM 199). We assumed that bankfull discharge and reach-average velocity were the same for the previous modelled times, (1850, 1895 and 1972). Bankfull depths, then, were calculated as:

$$H(t) = \frac{Q_0}{U_0 b(t)} \tag{5}$$

where, $H(t)$ and $b(t)$ are average bankfull depth and width, respectively, at each time, t (i.e. 1850, 1895 and 1972); and Q_0 and U_0 are bankfull discharge and average velocity, respectively, assumed constant. Annual USGS gauge records at Harrisburg verified both our measurement of width and estimated reach-average velocity.

Copyright © 2006 John Wiley & Sons, Ltd.

Table II. Input data for JP Model

Variable	Units	1850 value	1895 value	1972 value	Source
Width (B)	Metres (m)	160	235	185	Measured from channel planforms
Coefficient of Variation (COV) in Width	Percent (%)	34%	52%	39%	Computed from width measurements
Stage (H)	Metres (m)	2.75	1.87	2.37	Back-calculated from reach-average velocity
Bankfull Discharge (Qb)	Cubic metres per second (m^3/sec)	1190	1190	1190	Source: USACE, (2004)
Valley relief	Metres (m)	36	36	36	Measured from 10m DEM
Median grainsize (D_{50})	Metres (m)	0.039	0.039	0.039	Source: P. Klingeman, unpublished data

Parameters used to calculate near-bank flow velocity perturbation (U_b') for the 1850, 1895 and 1972 channels.

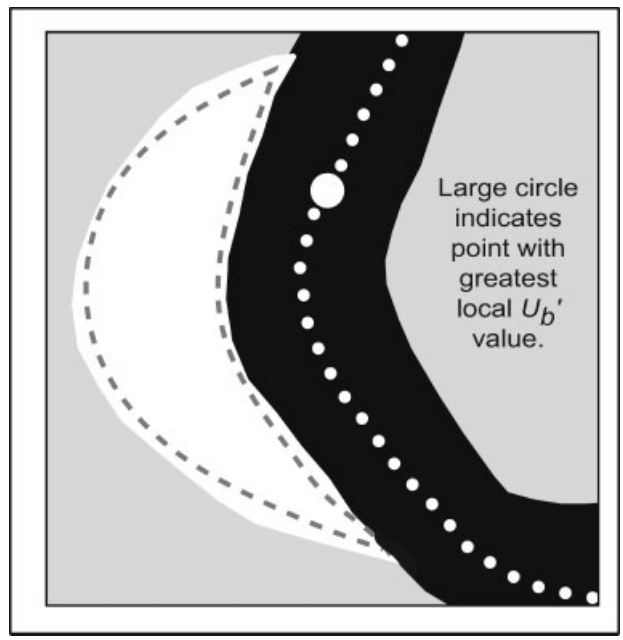

Figure 5. Overlaying bend polygons with U_b'. Each point has a corresponding near-bank velocity. We select the maximum U_b' for each bend and compute E_o by dividing U_b' by bank erosion rate

We overlaid bend-scale polygons with the centreline points and their associated velocities to verify that the sign and magnitude of U_b' correlate with bend geometry. Along large bends, the maximum U_b' generally occurs at or near the bend apex, while maximum U_b' for small bends often occurs near the apex of the next downstream bend but along the inside of the bend (Howard, 1992). In some cases, problems associated with our smoothing routine or planform irregularities caused U_b' to not correlate with bend geometry. Such cases were excluded from our analysis. Where U_b' does correlate with bend direction and curvature, we attribute the bend-scale polygon with the maximum U_b' associated with each polygon (Figure 5).

Calculating bank erodibility (E_o)

Once each polygon has an associated bank erosion rate and velocity perturbation, erodibility is calculated from Equation (2). Reach-average erodibilities for each material were obtained by averaging individual bend-scale E_o values for each bank material type for each time interval.

Copyright © 2006 John Wiley & Sons, Ltd.

To calculate E_o for Qalc and Qg2 we classified each bend-scale polygon with the type of bank material eroded. Bank material eroded for the period 1972–1995 was easily determined by overlaying channel maps, the Quaternary geological map of O'Connor *et al.* (2001), and aerial photographs in which the Qalc/Qg2 boundary is well defined. Bends influenced by bank stabilization structures between 1972–1995 were identified from digital maps of revetment produced by the PNWERC.

Classification of bank materials for the periods 1850–1895 and 1895–1932 required overlaying the geology map of O'Connor *et al.* (2001) with the channel maps and bend-scale polygons. Where the channel was positioned within the Holocene floodplain such that Qalc bordered both sides of the channel, bank material was classified as Qalc. For eastward-eroding bends near the floodplain border, channel maps from preceding time periods were overlain to determine whether the observed erosion occurred in areas that were previously mapped as floodplain features (e.g. side channel, active channel, island). If erosion through previous floodplain features was slight ($<$10 m) and no other evidence suggested Qalc was eroded, we assumed the bank material eroded was Qg2. Bends that appeared to migrate through some portion of relict floodplain features (Qalc) and Qg2, were excluded from our analysis. For all time periods, bend geometry and the direction of near-bank flow velocity as indicated by U_b' is used to classify bank material for stable bends ($<$5 m of erosion).

Limitations to the erodibility analysis

There are several potential sources of uncertainty associated with our bank erodibility analysis. We apply a single-thread, constant-width model to a multi-thread, variable-width stream. We assume erosion occurred under constant (bankfull) discharge, yet actual peak flows have fluctuated greatly over the 150-year study period. Uncertainty is introduced through historic data used to measure bank erosion rates and the input parameters and equations used to calculate near-bank flow velocities with the JP model. Our interpretation of E_o results is also influenced by the amount of channel we are able to analyse, as our analysis is only applicable in areas where we are able to link U_b' from channel geometry of the initial planform with erosion occurring over the interval. There is also uncertainty associated with classifying bank material eroded during historic time periods, as our classification routine may cause us to label some eroded areas as Qg2, although the actual eroded area may have been composed of Qg2 and Qalc. Although each of these topics is potentially important, we are only able to quantify uncertainty associated with our estimated bank erosion rates and address that issue here.

The historic channel maps from 1850, 1895 and 1932 contain error associated with mapping, georeferencing and digitization. While it is difficult to estimate uncertainty associated with survey techniques and active channel definition, we estimate absolute and relative errors for the 1850, 1895 and 1932 maps to be less than 10 m in magnitude (Table I). We estimate maximum error resulting from the georeferencing and digitization of aerial photographs to be between 5–10 m for the 1995 channel and 10 m for the 1972 channel. Thus each bank-erosion polygon could have up to 20 m of error associated with the actual distance migrated over the interval. For a bend that experienced significant erosion (e.g. 250 m) the maximum amount of uncertainty constitutes less than 10% of the distance migrated. Smaller bank-erosion polygons (e.g. 20 m of bank erosion) could have very high levels of uncertainty as the actual amount of erosion may range from 0–40 m.

RESULTS

Following criteria that resulted in exclusion of some parts of the channel from analysis, we were able to calculate bank erodibility along 36–61% of the channel during each time period (Table III). During earlier time periods, 1850–1895 and 1895–1932, many bends experienced avulsion or rapid migration such that the U_b' from the first time cannot be directly linked with observed erosion. Of the 96 bends analysed over all three study intervals, we excluded 44 bends due to planform discrepancies and three bends due to problems with U_b'. Although we are able to model 10–20 km of the floodplain, our sample sizes are low because E_o is calculated at the scale of 0.5–3 km long bends. During each time period, E_o is calculated for 3 to 13 bends per bank material.

Two-tailed *t*-tests (assuming unequal variance) were used to determine whether the mean E_o values for Qalc, Qg2 and revetment were statistically different from each other and to detect temporal changes in erodibility within bank materials (Table IV). The *t*-statistics reveal that the average E_o for Qalc was statistically different from Qg2 during

Copyright © 2006 John Wiley & Sons, Ltd.

Table III. Summary of bank erodibility results

Time period	% of channel length modelled[a]	Number of bends modelled			Reach averaged erodibility[b] (E_o)±1 std dev ($\times 10^{-7}$)			Coefficient of Variation (COV) in E_o values (%)			Average distance eroded (m)		
		Qalc	Qg2	Rvtmt[c]	Qalc	Qg2	Rvtmt	Qalc	Qg2	Rvtmt	Qalc	Qg2	Rvtmt
1850–1895	42	9	6	—	1.25 ± 0.52	0.27 ± 0.25	—	41	95	—	106	24	—
1895–1932	36	8	3	—	0.66 ± 0.42	0.36 ± 0.28	—	64	77	—	77	48	—
1972–1995	61	11	5	7	0.80 ± 0.41	0.17 ± 0.32	0.015 ± 0.028	51	195	190	47	4.3	2.2
All time periods	—	28	14	7	0.91 ± 0.50	0.25 ± 0.27	0.015 ± 0.028	55	109	190	75	22	

[a]Percentage approximates the length of channel for which we are able to link U_b' from the first time with erosion over the period. Centreline length is measured along the channel from the second time.
[b]Erodibility (E_o) is a dimensionless parameter obtained by dividing bank erosion rate (m/s) by near-bank flow velocity (m/s). Although erosion rates are measured in m/yr we convert the measured rates to m/s, which yields very low values ($\sim 10^{-7}$) with identical units as velocity.
[c]Of the 7 bends with revetment, 6 bends were composed of Qalc while Qg2 bordered 1 bend. Average E_o for Qalc with revetment was $0.017 \times 10^{-7} \pm 0.030$; the Qg2 revetted bend had E_o of 0.00.

Table IV. Significance levels (p-values) from students t-tests used to compare average E_o values across time periods and between bank materials

	1850–1895		1895–1932		1972–1995		
	Qalc	Qg2	Qalc	Qg2	Qalc	Qg2	Revetment
1850–1895 Qalc	X	3.4×10^{-4}	0.021	6.7×10^{-3}	0.048	4.3×10^{-4}	9.1×10^{-5}
1850–1895 Qg2	3.4×10^{-4}	X	0.050	0.66	4.9×10^{-3}	0.58	0.059
1895–1932 Qalc	0.021	0.050	X	0.21	0.50	0.036	3.3×10^{-3}
1895–932 Qg2	6.7×10^{-3}	0.66	0.21	X	0.084	0.41	0.17
1972–1995 Qalc	0.048	4.9×10^{-3}	0.50	0.084	X	7.6×10^{-3}	7.8×10^{-5}
1972–1995 Qg2	4.3×10^{-4}	0.58	0.036	0.41	7.6×10^{-3}	X	0.36
Revtmt	9.1×10^{-5}	0.059	3.3×10^{-3}	0.17	7.8×10^{-5}	0.36	X
All Time Periods	Qalc		Qg2		Rvtmt		
Qalc	X		2.4×10^{-6}		4.3×10^{-10}		
Qg2	2.4×10^{-6}		X		6.6×10^{-3}		
Revetment	4.3×10^{-10}		6.6×10^{-3}		X		

We computed the t-statistic using two-tailed t-test assuming unequal variance between samples. Lower values indicate lower probabilities that differences between average erodibilities are due to random chance.

1850–1895 and 1972–1995 ($p < 0.05$). Holocene alluvium from all periods was also statistically different from revetments ($p < 0.05$), however there was no meaningful difference between Qg2 and revetments ($p > 0.05$). Combining the average E_o values from all time periods reveals a 3-fold difference in E_o between Qg2 and Qalc, with higher significance levels than for individual time periods ($p \ll 0.05$). Temporal variation in average E_o was greater for Qalc than for Qg2 ($p \gg 0.05$ when comparing mean Qg2 E_o between each interval).

These t-test results suggest that although our sample populations are small and typically yield relatively high variability (Table III), there are distinct patterns of erodibility between bank materials and across time periods. During all time periods Qalc is, on average, 2–5 times more erodible than Qg2 (Table III and Figure 6). Revetted banks during the 1972–1995 period have very low erodibilities and are on average 11–84 times less erodible than Qg2 and Qalc. Average erodibility of Qalc decreased nearly 40% from the late-19th century to the late 20th century (Table III, Figure 6). Erodibility for Qg2 does not follow the same temporal trend, but small sample sizes make any changes statistically insignificant (Table IV). Of the three study periods, the interval 1895–1932 displays the lowest erodibility for Qalc and the highest for Qg2.

Copyright © 2006 John Wiley & Sons, Ltd.

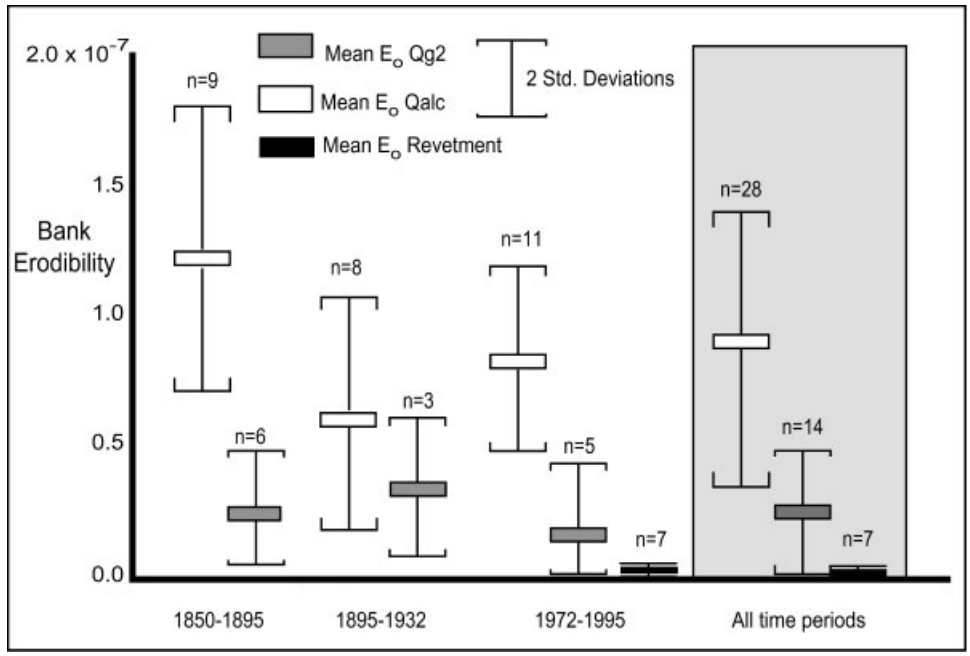

Figure 6. Bank Erodibility Trends for upper Willamette River 1850–1995. For all time intervals, Holocene Alluvium (Qalc) is on average 2–5 times more erodible than partially cemented Pleistocene Gravels (Qg2). Revetment installed along Qalc banks in the 1930's through 1970's is highly resistant to erosion

Longitudinal trends in erodibilities are associated with the distribution of resistant bank materials relative to the position of the Willamette River (Figure 7). There is a higher number of lower erodibility bends in the downstream portion of the reach (FPKM 185–198) where the Willamette has impinged upon Qg2 gravels bordering the eastern margin of the floodplain. Bends upstream of FPKM 200 are bordered by Qalc and generally have displayed higher erodibilities, though revetments cause diminished erodibilities along some bends of the 1972–1995 floodplain (e.g. FPKM 210).

The coefficient of variation (COV) for E_o increases over time for both Qalc and Qg2. Pleistocene gravels and revetments display greater variability than Holocene Alluvium during all time periods, as the COV for Qg2 is twice that of Qalc for 1850–1895 and 1972–1995, while COV for revetment is 3–4 times greater than Qalc. This variability between bank materials appears to be linked with systematic error associated with measuring bank erosion distances from historic maps and aerial photos.

For 1850–1895 and 1895–1932 time periods, the average distance eroded for modelled bends is approximately 70 m, whereas the average eroded distance for 1972–1995 is approximately 20 m (Table III). Assuming a maximum potential error of 20 m associated with each eroded distance, we estimate that E_o values from 1850–1895 and 1895–1932 may have up to 30% error while the smaller polygons from 1972–1995 yield much higher potential error, possibly as high as 90%. A similar relationship between eroded distance and error levels exists when comparing E_o values for Qalc against Qg2. On average, eroded distances for Qalc are 50–100 m, and therefore associated errors in E_o measurements could be as high as 20–50%. Average distances eroded for Qg2 are approximately 4–50 m and could have errors as great 40–300% (Table III). These preliminary error estimates generally agree with calculated COV values; bend populations with less erosion tend to have higher variability than populations with larger bank erosion distances.

During each time period, channel width varies by 30–50% of reach-averaged width and potentially introduces error in our calculation of U_b' and may therefore influence E_o values. We investigated the importance of channel width on E_o by varying channel width (and stage) in the JP model and overlaying the adjusted U_b' values on our bend-scale polygons. For each 10% increase in channel width, bend-scale E_o decreased by about 10%, whereas a 10% decrease in channel width generally caused bend-scale E_o to increase by 14%. As channel width along most of

Copyright © 2006 John Wiley & Sons, Ltd.

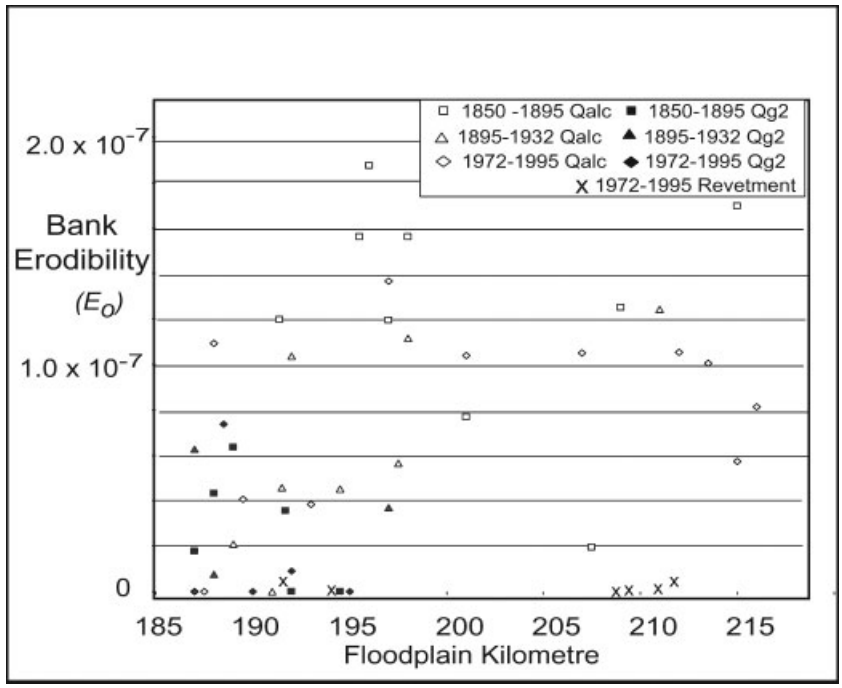

Figure 7. Longitudinal patterns in bank erodibility 1850–1995. Holocene alluvium (Qalc) has historically been more erodible than Pleistocene gravels (Qg2), though there are several Qalc bends in the lower reach (FPKM 185–195) with lower erodibilities than those in the upper reach. Bends stabilized with revetments in the mid-20th century have very low erodibilities

our modelled bends varies by 10–20% of the reach-averaged width for that time period, error in our computed E_o due to planform fluctuation is probably on the order of 10–15%. Our sensitivity trials also revealed that near-bank flow velocity is most sensitive to planform irregularities and that while adjustments in width to depth ratios and discharge influenced the magnitude of U_b', the relative difference in maximum U_b' between individual bends remained similar.

DISCUSSION

Applicability of a bank erosion analysis to the upper Willamette

Our analysis demonstrates that differences in erodibility due to bank materials can be detected at the scale of individual bends using a meander migration model and historic channel maps. The primary premise of the analysis is that, for single-thread, constant-width channels, bank erosion is a continuous process resulting from near-bank velocity and bank erodibility. On the historically anastomosing upper Willamette, application of such an analysis requires careful selection of reaches that best meet these assumptions. By excluding avulsions and avulsion-related migration, both of which primarily occurred along anastomosed reaches, we focus our study on single-thread areas that evolved through lateral migration. We further restrict our analysis to bends where channel planform from the first time is a good predictor of the actual lateral migration that occurred over the time interval.

The remaining assumptions of our meander migration model prove more problematic as the analysis assumes that bank erosion occurs at a constant rate, along constant width rivers characterized by constant (bankfull) discharge. Along the upper Willamette channel width and presumably, discharge, varies as the channel alternates between multi-thread and single thread reaches. Because the channel has adopted a more single-thread planform in the 20th century, the effect of multiple channels on apparent erodibility was probably greatest in the period 1850–1895 and increasingly less important in the intervals 1895–1932 and 1972–1995. Even as greater portions of the

Copyright © 2006 John Wiley & Sons, Ltd.

upper Willamette have become single-thread, channel width is variable, (Table II), which potentially introduces error in our calculations of U_b' and E_o.

Our calculation of bank erodibility is based on estimated values of near-bank velocity, therefore the ability of the JP model to correctly compute variation in velocity perturbation due to channel curvature is critical to our analysis. Assessing the ability of the JP model to correctly estimate U_b' is difficult and would entail either forward modelling, in which we compared predicted migration against actual erosion, or comparison of simulated U_b' and actual near-bank velocity measurements taken at bankful discharge. In the absence of such comparisons we rely upon our own examination of model results and past studies to evaluate the ability of the JP model to predict channel migration.

We use the JP model to predict which bends are likely to migrate more rapidly than others based on channel curvature. For this reason, we are less concerned with local U_b' calculated at each point along the centreline and more concerned with bend-scale patterns in computed curvature and near-bank velocity. We evaluated the performance of the JP model by examining each bend and determining whether the model was able to correctly predict (a) which bank was likely to experience the greatest magnitude of near-bank velocity; (b) the general location of maximum U_b' relative to overall bend geometry; and (c) the location of maximum U_b' relative to actual erosion for that time interval. We found that along areas subject to moderate lateral migration (e.g. less than 300 m of erosion) the JP model was generally able to meet each of these criteria. Areas where the JP did not perform adequately were typically bends excluded from our analysis for other reasons, such as rapid migration or migration influenced by avulsion.

While rapid migration of bends is within the conceptual realm of model predictability, in practice rapid migration results in such large planform changes over the periods examined that the initial planforms do not provide sufficient information to predict such large changes. For example, many low-sinuosity sections of the 1895 channel developed into bends that subsequently migrated downstream, producing a more sinuous channel by 1932. The low-sinuosity sections of the 1895 channel have very low U_b' values, suggesting that small initial bends may have formed slowly, but later migrated more rapidly once sufficient curvature was established to drive higher near-bank velocities. Our analysis of historic erosion along the Willamette River floodplain is therefore biased towards bends with relatively low migration rates, as we exclude nearly half of the entire bend population over the three time periods due to rapid migration. If rapid migration were partly or wholly due to high erodibilities, then our estimate of E_o would be biased towards lower values. It seems just as likely, however, that the observed rapid migration is entirely driven by characteristics of the planform.

Our evaluation of the JP model is consistent with previous studies, which found that the model was generally able to simulate realistic meander migration. The primary problems encountered by other authors were found when using the model to predict channel migration rather than simply using it to compare maximum U_b' between bends. For example, (Lancaster and Bras, 2002) found that the simulated bends were overly smooth in comparison to natural rivers and the model did not produce more complicated bend shapes, such as double-headed meander bends. Johannesson and Parker (1985) found that an earlier version of the model required extensive calibration in order to determine proper bank-erodibility values necessary for correct prediction of channel migration. In the absence of such calibration, Garcia *et al.* (1994) found that an earlier version of the JP model was better at predicting the downstream migration of bends than outward erosion.

Ability of a simple analysis to detect differences in erodibility due to bank materials

Although our sample sizes are limited and significance levels in each time period are modest, consistent differences in relative erodibility between bank materials over all time periods boosts our confidence in the E_o results from individual time periods. In each time period, Holocene alluvium is on average 2–5 times more erodible than Pleistocene gravels. Moreover, by averaging E_o across all time periods, we detect a three-fold difference in E_o between Qalc and Qg2 and gain a much higher significance level than for individual periods.

Initially, we anticipated greater differences in erodibility between bank materials because casual field observations suggested Holocene alluvium was much less consolidated than partially-cemented Qg2 gravels. The relatively modest difference in bank erodibility as detected in our analysis may be due in part to vegetation, which exerts a greater influence on Qalc surfaces because few plant species have roots that are able to extend through the 3–5 m of Missoula Flood deposits overlying Qg2. Additionally, because Qg2 is typically exposed along steep (near

Copyright © 2006 John Wiley & Sons, Ltd.

vertical) banks, very little bank roughness is contributed by vegetation. In contrast, Qalc banks are more directly influenced by vegetation as bank height is typically less than 3 m and overlying alluvial soils are more conducive to plant growth. In the 19th century, the Holocene floodplain was densely forested, and though much of the modern floodplain has been converted to agriculture, there is still considerable riparian vegetation bordering the channel along Qalc banks.

Previous studies have shown vegetation to reduce bank erosion by increasing soil tensile strength, mass loading, and bank roughness (Thorne, 1990; Thorne and Furbish, 1995; Micheli and Kirchner, 2002; Simon and Collison, 2002). However, feedbacks between wood, sediment and floods have also been shown to trigger dynamic floodplain behaviour including avulsions, bank attack and secondary channel formation (Keller and Swanson, 1979; Swanson and Lienkaemper, 1982; Fetherston *et al.*, 1995; O'Connor *et al.*, 2003). Although the riparian vegetation and land conversion may have had an important effect on channel change along the Willamette River, we do not have sufficient vegetation data to determine that effect. Moreover, historic trends in flow regime might obscure trends in land use. For example, decreased flow due to dams might decrease apparent erodibility, but decreased bank vegetation might increase apparent erodibility. Such scenarios would be consistent with the results of our analysis.

Variability in calculated values of E_0 seems most closely linked with error arising from our measurements of erosion distance. Bends with less erosion (e.g. <20 m) have much higher levels of uncertainty than bends that experienced greater levels of erosion (e.g. >100 m). Therefore time periods or bank materials that experienced small amounts of erosion are likely to have very high levels of uncertainty (often exceeding 100% of the computed E_o for that bend). This relationship between erosion distance and uncertainty may partially explain the high levels of variation associated with Qg2, which has coefficients of variation ranging from 77–170% whereas variation for Qalc is typically lower (40–70%). Although it is difficult to quantify total error associated with the JP model, we estimate that time periods having higher levels of variation in reach-average channel width are more likely to have higher error in U_b' and thus E_o.

The effect of floodplain variables such as sediment properties and riparian vegetation on bank erodibility is more difficult to quantify. Within both Qalc and Qg2, heterogeneity in consolidation, grainsize or bank height may cause some areas within each bank material to be more erodible than other areas. For instance, some areas of the upper Willamette floodplain are bordered by erodible Holocene Alluvium, yet they experience little to no bank erosion and have low apparent erodibilities. Nearly one-half of Qalc bends in the 1895–1932 interval, and about one-fourth of Qalc bends in the 1972–1995 interval display lower erodibilites along reaches where the channel alternates between Qalc and Qg2 banks in the lower study reach. Because we have relatively small sample sizes, each of these lower-erodibility Qalc bends have a potentially important effect on reach-average erodibility. The reason for low erodibility is unclear and may be due to over-estimation of U_b', vegetation or intrinsic differences in local erodibility. It is also possible that certain bends bordered by erodible material may experience 'secondary stabilization' in which resistant banks along adjacent bends impart some level of local stability.

While our analysis has shown that measurable differences in bank erodibility have persisted over the last century, the logical next step is to conduct field-based tests in order to quantify actual bank material strength properties. If conducted at the low-water line, such tests may reveal absolute differences in bank strength between partially-cemented Pleistocene gravels and Holocene alluvium and could also be used to determine the influence of riparian vegetation on bank strength. Simulation modelling of channel migration through various bank materials may be used to explore the effect of revetment removal or to discern whether resistant banks can exert a stabilizing influence on adjacent bends.

Implications of resistant bank materials

Throughout most of the 20th century, portions of channel flowing against Qg2 gravels generally do not migrate away from Qg2. Rather, as meander migration continues, bend enlargement causes greater portions of the channel to flow against Qg2 gravels. This pattern of steady increases in the percentage of Qg2 banks was not always the case. Between 1850–1895, avulsions and migration led to increases in the length of channel bordered by Qg2 (Figure 2), but during the interval 1895–1932 rapid migration and bend cut-off allowed several bends to migrate away from Qg2. We also observe that, prior to flow regulation, greater, more erosive flows and erodible banks allowed low-sinuosity reaches to develop bends that migrated rapidly downstream, triggering further channel

Copyright © 2006 John Wiley & Sons, Ltd.

change. Presently, revetments placed along Holocene alluvium restrict lateral migration and prevent avulsions. The combination of naturally resistant banks, revetment and flood control causes stabilization of much of the modern Willamette.

While channel migration may result in economic losses due to property damage, channel movement has also been shown to have beneficial consequences for riparian-zone ecosystems. Bank erosion contributes sediment and large-wood to the river that can be deposited downstream leading to formation of bars and islands (Swanson and Lienkaemper, 1982; Gurnell *et al.*, 2001; O'Connor *et al.*, 2003). Migration leaves behind newly deposited gravel bars that allow for recruitment of pioneer vegetation species and over time provides a mosaic of geomorphic surfaces that increase the diversity of riparian habitat (Fetherston *et al.*, 1995). Frequent reworking of floodplain sediments and redistribution of bed material enhances hyporheic flows, which support cooler stream temperatures and habitat for benthic organisms (Wondzell and Swanson, 1996; Fernald *et al.*, 2001).

Efforts aiming to increase channel migration should focus on removing bend-size portions of the Willamette from resistant bank materials. As banks composed of Holocene alluvium are intrinsically more erodible than Pleistocene gravels, removing revetment from these bends may produce higher levels of migration than would be gained by removing revetments from Pleistocene gravels. Analysis of historic migration indicates that Qalc banks upstream of floodplain kilometre 200 tended to have higher levels of erodibility than banks in the lower study reach where bends alternate between Qalc and Qg2. Although more investigation is required to determine if there are significant differences in bank erodibility within Qalc, migration along upstream areas may be greater than for bends in the lower study reach. Historic patterns of channel change also indicate that even relatively low-sinuosity reaches bordered by erodible bank materials can display dynamic meander behaviour. However, rapid migration may be due in part to flow regime and there may be a minimum bend length required for such behaviour to develop. Thus, further investigation is needed to more fully understand meander migration along the upper Willamette.

CONCLUSION

Although bank erosion results from complex relationships between flow and floodplain characteristics, our simple model of bank erodibility reveals distinct patterns of erodibility linked to bank materials. Across three time periods spanning more than 100 years, we find that Holocene alluvium is on average 2–5 times more erodible than Pleistocene gravels. When erodibility values from all time periods are combined, significance levels are much higher, revealing that Holocene alluvium is about three times more erodible than Pleistocene gravels, which in turn are at least 11 times more erodible than revetments.

In the century following Euro-American settlement, the length of channel flowing against naturally resistant Qg2 gravels has steadily increased. Approximately 30% of the Willamette is presently stabilized by moderately resistant Qg2 gravels, while more than 40% is stabilized by highly resistant revetment. Even along bends bordered by erodible Holocene alluvium, migration rates may be low, as local variation in bank materials or vegetation may exert a stabilizing influence on bank erodibility. Our analysis also reveals that migration rates are further influenced by planform, which can exert large influences on channel movement irrespective of bank material. The role of resistant bank materials on channel migration may be further explored through bank material strength tests and simulation modelling, both of which may provide absolute differences in bank erodibility for Holocene alluvium and Pleistocene gravels and may quantify the role of riparian vegetation on bank erosion. These results suggest that restoration efforts aiming to increase channel migration should focus on removing revetment from bend-size reaches bordered by Holocene alluvium.

ACKNOWLEDGEMENTS

We thank Stan Gregory, Linda Ashkenas, Randy Wildman and other members of the Pacific Northwest Ecosystem Research Consortium whose previous work and expertise greatly enhanced this study. We also thank Jim O'Connor for providing insight on Willamette Valley stratigraphy and field equipment. We thank Gordon Grant and Andrew Meigs for guidance and helpful reviews of this document. This work was supported by the National Science Foundation (Biocomplexity Grant 0120022).

Copyright © 2006 John Wiley & Sons, Ltd.

APPENDIX

JOHANNESSON & PARKER (1989) MODEL OF NEAR-BANK VELOCITY PERTURBATION (U'_b)

The Johannesson & Parker (1989) model assumes that U'_b is largely driven by channel curvature:

$$U'_b = \chi_{20} UBC(s) + \frac{C_f UB^2}{H}\left[\chi_{20}\left(\frac{U^2}{gH}+2\right)-1\right]e^{\frac{-2C_f s}{H}}\int_0^s C(s')e^{\frac{-2Cfs'}{H}}ds' + \frac{C_f UB}{H}(K+A_s)e^{\frac{-2Cfs}{H}}\int_0^s C(s')e^{\frac{2Cfs'}{H}}ds' \quad \text{(A1)}$$

We have made several adaptations to the JP model to make the model more representative of the Willamette River. We have substituted local curvature, C, for the effective curvature integral in the argument of the second integral of Equation (A1) and we use Ikeda's (1989) equation for transverse bedslope to calculate K in Equation (A7).

Coefficients used in the JP model:

χ_{20}, χ_1, χ	Coefficients used to describe secondary flow given by: $\chi_{20} = \frac{1}{\chi_1^3}\left(\chi^3 + \chi^2 + \frac{2\chi}{5} + \frac{2}{35}\right)$, $\chi_1 = \frac{0.077}{\sqrt{C_f}}$, $\chi_1 = \frac{0.077}{\sqrt{C_f}} - \frac{1}{3}$	(A2-4)
U,B,H	Reach-average velocity, channel width and stage for bankfull discharge; described in Table 2	
$C(s)$	Channel curvature at distance s along the centreline	
s'	Distance to point upstream from s	
C_f	Coefficient of friction, calculated as: $C_f = \frac{gHS}{U^2}$, where g is gravitational constant and S is channel slope	(A5)
A_s	Coefficient used to describe bed topography, calculated as: $A_s = \frac{181}{\chi_1}\left(\frac{2H}{B}\right)^2\left(2\chi^2 + \frac{4\chi}{5} + \frac{1}{15}\right)$	(A6)
K	Coefficient used to calculate transverse bedslope in gravel-bed rivers, from Ikeda (1989): $K = \sqrt{\frac{\psi}{\psi_{cr}}}\left(\frac{0.2278}{\sqrt{C_f}} - 0.3606\right)$	(A7)

REFERENCES

Balster CA, Parsons RB. 1968. Geomorphology and Soils, Willamette Valley, Oregon. Special Report 265, Agricultural Experiment Station, Oregon State University, Corvallis.

Balster CA, Parsons RB. 1969. Late Pleistocene stratigraphy, southern Willamette Valley, Oregon. *Northwest Science* **43**: 116–129.

Dykaar BB, Wigington PJ. 2000. Floodplain formation and cottonwood colonization patterns on the Willamette river, Oregon, USA. *Environmental Management* **25**(1): 87–104.

Fernald AG, Wigington PJ, Landers DH. 2001. Transient storage and hyporheic flow along the Willamette river, Oregon: field measurements and model estimates. *Water Resources Research* **37**(6): 1681–1694.

Fetherston KL, Naiman RJ, Bilby RE. 1995. Large woody debris, physical process, and riparian forest development in montane river networks of the Pacific Northwest. *Geomorphology* **13**: 133–144.

Garcia MH, Bittner L, Nino Y. 1994. Mathematical modeling of meandering streams in Illinois; A tool for stream management and engineering. Hydraulic Engineering Series 43, Illinois Water Resources Center, Urbana, Illinois.

Glen JL. 1965. Late Quaternary sedimentation and geological history of the north Willamette Valley, Oregon. Ph.D. Thesis, Oregon State University, Corvallis, p. 231.

Gregory S, Ashkenas L, Oetter D. 2000. Willamette River, Oregon, Active Channel 1995. http://www.fsl.orst.edu/pnwerc/wrb/access.html [20 October 2003].

Gregory S. *et al*. 2002. Revetments. In *Willamette Valley Planning Atlas*, Hulse D, Gregory S, Baker J (eds). Oregon State University Press: Corvallis; p. 178.

Copyright © 2006 John Wiley & Sons, Ltd.

Gurnell AM, Petts GE, Hannah DM. 2001. Riparian vegetation and island formation along the gravel-bed Riume Tagliamento, Italy. *Earth Surface Processes* **26**: 31–62.

Howard AD. 1992. Modeling channel migration and floodplain sedimentation in meandering streams. In *Lowland Floodplain Rivers: Geomorphical Perspectives*, Carling P, Petts G (eds). John Wiley & Sons Ltd, Chinchester; p. 302.

Hulse D, Gregory S, Baker J (eds). 2002. *Willamette River Basin Planning Atlas; Trajectories of Environmental and Ecological Change*, 2 Oregon State University Press: Corvallis; p. 178.

Ikeda S. 1989. Sediment transport and sorting at bends. In *River Meandering*, Ikeda S, Parker G (eds). American Geophysical Union: Washington, D.C.; pp. 103–126.

Ikeda S, Parker G, Sawai K. 1981. Bend theory of river meanders, part 1: linear development. *Journal of Fluid Mechanics* **112**: 363–377.

Johannesson H, Parker G. 1985. Computer simulated migration of meandering rivers in Minnesota. Project Report 242, St. Anthony Falls Hydraulic Laboratory, University of Minnesota, Minneapolis.

Johannesson H, Parker G. 1989. Velocity redistribution in meandering rivers. *Journal of Hydraulic Engineering* **115**(8): 1019–1039.

Keller EA, Swanson FJ. 1979. Effects of large organic material on channel form and fluvial process. *Earth Surface Processes and Landforms* **4**: 361–380.

Lancaster S, Bras R. 2002. A simple model of river meandering and its comparison to natural channels. *Hydrological Processes* **16**(1): 1–26.

Landers DH, Fernald AG, Andrus C. 2002. Off-channel habitats. In *Willamette River Basin Planning Atlas*, Hulse D, Gregory S, Baker J (eds). Oregon State University Press: Corvallis, Oregon; p. 178.

Micheli E, Kirchner J. 2002. Effects of wet meadow riparian vegetation on streambank erosion. 1. Remote sensing measurements of streambank migration and erodibility. *Earth Surface Processes and Landforms* **27**: 627–639.

Micheli ER, Kirchner JW, Larsen EW. 2004. Quantifying the effect of riparian forest versus agricultural vegetation on river meander migration rates, central Sacramento River, California, USA. *River Research and Applications* **20**(5): 537–548.

Nanson GC, Hickin EJ. 1986. A statistical analysis of bank erosion and channel migration in western Canada. *Geological Society of America Bulletin* **97**(4): 497–504.

O'Connor JE, Sarna-Wojcicki A, Wozniak KC, Polette DJ, Fleck RJ. 2001. Origin, extent, and thickness of Quaternary geologic units in Willamette Valley, Oregon. Professional Paper 1620, U.S. Geological Survey, Reston, Virginia.

O'Connor JE, Jones MA, Haluska TL. 2003. Floodplain and channel dynamics of the Queets and Quinalt rivers. Washington, USA. *Geomorphology* **51**: 31–59.

Oregon Climate Service. 2004. The Climate of Oregon. http://www.ocs.orst.edu/ocs.shtml [3 January 2004].

Reckendorf FF. 1973. Techniques for Identifying Flood Plains in Oregon. Ph.D Thesis, Oregon State University, Corvallis, p. 344.

Simon A, Collison AJC. 2002. Quantifying the mechanical and hydrologic effects of riparian vegetation on streambank stability. *Earth Surface Processes and Landforms* **27**: 527–546.

Swanson FJ, Lienkaemper GW. 1982. Interactions among fluvial processes, forest vegetation, and aquatic ecosystems, South Fork Hoh River, Olympic National Park. In *Ecological Research in National Parks of the Pacific Northwest, Proceedings from Second Conference on Scientific Research in the National Parks, San Francisco CA*, Starkey EE, Franklin JF, Matthews JW (eds). Oregon State University Forest Research Laboratory: Corvallis, Oregon; pp. 30–34.

Thorne CR. 1990. Effects of vegetation on riverbank erosion and stability. In *Vegetation and Erosion*, Thornes JB (ed.). John Wiley and Sons: Chichester; pp. 125–144.

Thorne SD, Furbish DJ. 1995. Influences of coarse bank roughness on flow within a sharply curved river bend. *Geomorphology* **12**: 241–257.

USACE. 1867–1892. Annual Reports of Chief of Engineers. United States Army Corps of Engineers, Washington, D.C.

USACE. 1875. Annual Report of Chief of Engineers. United States Army Corps of Engineers, Washington, D.C.

Wallick JR. 2004. Geology, flooding and human activities: establishing a hierarchy of influence for controls on historic channel change, Willamette River, Oregon. M.S. thesis, Oregon State University, Corvallis; p. 171.

Willingham WF. 1983. *Army Engineers and the Development of Oregon*. USACE: Portland; p. 259.

Wondzell SM, Swanson FJ. 1996. Seasonal and storm dynamics of the hyporheic zone of a 4th-order mountain stream, II, Nitrogen cycling. *Journal of the North American Benthological Society* **15**(1): 20–34.

Copyright © 2006 John Wiley & Sons, Ltd.